ELSEVIER

NeuroImage

www.elsevier.com/locate/ynimg
NeuroImage 41 (2008) 690–698

Positron emission tomography imaging using an inverse agonist radioligand to assess cannabinoid CB_1 receptors in rodents

Garth Terry,[a,c] Jeih-San Liow,[a] Eyassu Chernet,[b] Sami S. Zoghbi,[a] Lee Phebus,[b] Christian C. Felder,[b] Johannes Tauscher,[b] John M. Schaus,[b] Victor W. Pike,[a] Christer Halldin,[c] and Robert B. Innis[a,*]

[a]*Molecular Imaging Branch, National Institute of Mental Health, Bethesda, MD, USA*
[b]*Lilly Research Laboratories, Lilly Corporate Center, Indianapolis, IN, USA*
[c]*Karolinska Institutet, Department of Clinical Neuroscience, Psychiatry Section, Stockholm, Sweden*

Received 4 September 2007; revised 17 January 2008; accepted 1 March 2008
Available online 18 March 2008

[^{11}C]MePPEP is an inverse agonist and a radioligand developed to image cannabinoid CB_1 receptors with positron emission tomography (PET). It provides reversible, high specific signal in monkey brain. We assessed [^{11}C]MePPEP in rodent brain with regard to receptor selectivity, susceptibility to transport by P-glycoprotein (P-gp), sensitivity to displacement by agonists, and accumulation of radiometabolites. We used CB_1 receptor knockout mice and P-gp knockout mice to assess receptor selectivity and sensitivity to efflux transport, respectively. Using serial measurements of PET brain activity and plasma concentrations of [^{11}C]MePPEP, we estimated CB_1 receptor density in rat brain as distribution volume. CB_1 knockout mice showed only nonspecific brain uptake, and [^{11}C]MePPEP was not a substrate for P-gp. Direct acting agonists anandamide (10 mg/kg), methanandamide (10 mg/kg), CP 55,940 (1 mg/kg), and indirect agonist URB597 (0.3 and 0.6 mg/kg) failed to displace [^{11}C]MePPEP, while the inverse agonist rimonabant (3 and 10 mg/kg) displaced >65% of [^{11}C]MePPEP. Radiometabolites represented ~13% of total radioactivity in brain between 30 and 120 min. [^{11}C]MePPEP was selective for the CB_1 receptor, was not a substrate for P-gp, and was more potently displaced by inverse agonists than agonists. The low potency of agonists suggests either a large receptor reserve or non-overlapping binding sites for agonists and inverse agonists. Radiometabolites of [^{11}C]MePPEP in brain caused distribution volume to be overestimated by ~13%.
Published by Elsevier Inc.

Introduction

The cannabinoid type 1 (CB_1) receptor is the most abundant G-coupled protein receptor in brain known to date and is involved in multiple neuromodulatory pathways (Grotenhermen, 2005, Pacher et al., 2006). In addition, the CB_1 receptor is associated with addictive behaviors (alcohol, drugs, and food) and is now an active target for medication development (Xie et al., 2007). For example, rimonabant, a CB_1 receptor inverse agonist, was recently approved in Europe for appetite reduction and weight loss (Van Gaal et al., 2005).

Effective PET radioligands for CB_1 receptors have potential to guide dosing of therapeutic agents and to act as biomarkers in the study of physiology and pathophysiology. For example, Burns et al. (2007) reported the synthesis of a novel PET radioligand for the CB_1 receptor and its use to measure receptor occupancy in monkeys and humans. We also developed a promising PET radioligand for the CB_1 receptor, [^{11}C]MePPEP ((*3R,5R*)-5-(3-methoxy-phenyl)-3-((*R*)-1-phenyl-ethylamino)-1-(4-trifluoromethyl-phenyl)-pyrrolidin-2-one) (Yasuno et al., 2008). MePPEP is a high potency inverse agonist with selectivity for CB_1 (K_b=0.6 nM) *vs.* CB_2 (K_b=360 nM) receptors. Despite its moderately high lipophilicity (Log$D_{7.4}$=4.8), [^{11}C]MePPEP shows good brain uptake and a high percentage (>85%) of specific binding in monkey brain (Yasuno et al., 2008). We sought to evaluate further this promising radioligand in rodents, using invasive procedures and transgenic animals that are difficult or unavailable in primates.

Rodents allowed two important parameters to be investigated that would be difficult to measure in primates. First, after euthanizing rats and extracting radioactivity, we measured radiometabolites in brain and assessed their impact on PET measurements and data analysis. Compartmental modeling is the "gold standard" method to analyze serial PET measurements of brain radioactivity

* Corresponding author. National Institute of Mental Health/National Institutes of Health, Molecular Imaging Branch, 31 Center Drive, Room B2-B37, MSC 2035 Bethesda, MD 20892-2035, USA. Fax: +1 301 480 3610.
E-mail address: robert.innis@nih.gov (R.B. Innis).
Available online on ScienceDirect (www.sciencedirect.com).

1053-8119/$ - see front matter. Published by Elsevier Inc.
doi:10.1016/j.neuroimage.2008.03.004

and plasma concentrations of parent radioligand. The typical outcome measure is distribution volume, which is proportional to the density of receptors and the affinity of the radioligand (Innis et al., 2007). Compartmental analysis typically assumes that the radioactivity measured by PET represents only parent radioligand. If so, then stable values of distribution volume over time will be obtained after a minimal period of image acquisition (e.g., 20–60 min). If estimates of distribution volume continuously increase with longer durations of data acquisition, one suspects either the accumulation of radiometabolites in brain or a failure of the radioligand to reach equilibrium in brain and plasma.

Second, rodents allowed us to administer very high doses of drugs to assess the differential potency of agonist and inverse agonists to displace radioligand binding. We found that an inverse agonist, rimonabant, potently displaced [^{11}C]MePPEP binding in brain. In contrast, high and, in some cases, lethal doses of an agonist failed to displace any significant radioligand binding in brain.

Materials and methods

Anandamide (arachadonoyl ethanolamide), methanandamide ((*R*)-(+)-arachidonyl-1'-hydroxy-2'-propylamide), and URB597 ((3'-(aminocarbonyl)[1,1'-biphenyl]-3-yl)-cyclohexylcarbamate) were purchased from Cayman Chemical (Ann Arbor, MI). CP 55,940 (5-(1,1-dimethylheptyl)-2-[(1R,2R,5R)-5-hydroxy-2-(3-hydroxypropyl)cyclohexyl]-phenol) was purchased from Tocris Bioscience (Ellisville, MO). Rimonabant, MePPEP, and *O*-desmethyl-MePPEP were synthesized at Eli Lilly and Company (Indianapolis, IN).

Animals

Male Sprague–Dawley rats (346±68 g) and age-matched P-gp knockout (*mdr-1a/1b*(−/−)) (Schinkel et al., 1996) and wild type mice (*mdr-1a/1b*(+/+), 27.7±4.7 g) were purchased from Taconic Farm (Germantown, NY, USA). Dr. George Kunos (National Institute of Alcohol Abuse and Alcoholism) provided the CB_1 receptor knockout mice.

Synthesis of [^{11}C]MePPEP

[^{11}C]MePPEP was prepared from the desmethyl precursor and [^{11}C]iodomethane, as previously described in Yasuno, et al. (2008).

Preparation for PET scanning

All rodents were anesthetized with 1.5% isoflurane in 100% oxygen, and body temperatures were maintained between 36.5 and 37.0 °C with a heating pad or lamp. Intravenous injections were performed via polyethylene cannulae (PE-10; Becton Dickinson, NJ, USA) in the mouse tail or rat penile vein. The cannulae were secured with tissue adhesive (Vetbond; 3M, St. Paul, MN, USA). To measure the concentration of [^{11}C]MePPEP in serial blood samples, an arterial cannula was placed in the femoral artery of each of four rats (332±67 g). After [^{11}C]MePPEP injection, arterial pressure caused a continuous flow of blood which was collected as 6 samples of ~200 μL each for the first 3 min. Afterwards, samples of 200 μL were collected at 5 and 10 min; 500 μL at 25, 40, and 60 min; and ~3 mL at the end of the 2-hour scan.

PET imaging

The Advanced Technology Laboratory Animal Scanner (Seidel et al., 2003) can accommodate a single rat or a pair of mice, for which we typically paired a wild type and knockout mouse. Serial dynamic scans began at the time of injection and continued for 100 min with frames of 6×20 s, followed by 5×1, 4×2, 3×5, 3×10, and 2×20 min. Images were reconstructed by a 3D ordered-subset expectation maximization algorithm into 17 coronal slices with 3 iterations, resulting in a resolution of about 1.6 mm full width at half maximum (Johnson et al., 2002, Liow et al., 2003). The data were not corrected for attenuation or scatter.

Tomographic images were analyzed with pixel-wise modeling computer software (PMOD Technologies Adliswil, Switzerland). Regions of interest were identified relative to a rat (Paxinos and Watson, 1998) or mouse (Paxinos and Franklin, 2001) brain stereotactic atlas. Radioactivity was decay-corrected to time of injection and expressed as percent standardized uptake value (% SUV), which normalizes for injected activity and body weight.

$$\%\text{SUV} = [(\text{activity per g tissue})/(\text{injected activity})] \times \text{g body weight}$$

Displacement of [^{11}C]MePPEP with cannabinoid agents

All pharmacological challenges were administered at 40 min after radioligand injection, which was between 15 and 20 min after peak uptake. Rimonabant (3 mg/kg, IV) was administered in a dose known to displace [^{11}C]MePPEP in monkey brain (Yasuno et al., 2008). We selected doses of agonist agents that are known to have central nervous system activity as measured with behavior or with levels of anandamide, the primary endogenous agonist for CB_1 in the brain (Fride and Mechoulam, 1993, Abadji et al., 1994, McGregor et al., 1996, Piomelli et al., 2006). URB597 is an indirect acting agonist, because it inhibits both fatty acid amide hydrolase (FAAH), an enzyme that metabolizes anandamide, as well as the anandamide transporter (Dickason-Chesterfield et al., 2006). The dose of URB597 used (0.3 mg/kg IP) was reported to cause FAAH inhibition within 15 min and increase brain levels of anandamide >3 fold within 60 min (Piomelli et al., 2006). Therefore, two animals were administered URB597 at 40 min after radioligand injection to parallel the other agonist challenges, and another animal was administered URB597 at 1 h before the radioligand injection to achieve maximal and prolonged inhibition of FAAH. To ascertain if URB597 did not increase endogenous anandamide sufficiently, or if injected anandamide was rapidly metabolized, we pretreated two rats with URB597 and administered anandamide at 40 min after radioligand injection.

Ex vivo mass spectrometry

The mass spectrometry experiments used a novel technique in which the reporter molecule (MePPEP) was injected at low doses and subsequently measured in brain extracts with mass spectrometry (Chernet et al., 2005). The animals were pretreated with pharmacological doses (e.g., 10 mg/kg IV) of displacing agents 15 min before being injected with MePPEP (30 μg/kg IV). The animals were euthanized 60 min later and the concentration of MePPEP was measured in brain extracts with mass spectrometry.

The mass spectrometry experiments were performed at Eli Lilly (Indianapolis, IN) and are described below. Rimonabant or CP

55,940 was in a vehicle comprised of intralipid (Sigma Chemical Co. St. Louis, MO) containing 0.2% acetic acid. MePPEP (1 mg) was dissolved in 1 mL of intralipid containing 1% acetic acid, diluted with sterile water to a final concentration of 30 μg/mL, and administered to rats in a volume of 1 mL/kg.

Adult male Sprague–Dawley rats (225–250 g; Harlan Sprague–Dawley, Indianapolis, IN) were used without anesthesia. Vehicle, rimonabant (10 mg/kg), or CP 55,940 (1 mg/kg) was administered by tail vein IV to groups of 3 rats, and MePPEP (30 μg/kg IV) was administered 15 min later. Rats were sacrificed 1 h later by cervical dislocation. A portion of each frontal cortex was dissected, weighed, and placed in centrifuge tube on ice. Brain tissues were homogenized using a cell disrupter in four volumes (W/V) of acetonitrile containing 0.1% formic acid. To extract the tracer (*i.e.*, MePPEP), tissues were centrifuged at 20,000 ×*g* for 14 min. Aliquots of supernatant containing the tracer were diluted with water to an acetonitrile content less than that of the mobile phase and injected by auto sampler onto an HPLC employing a Zorbax SB-C18, 2.1×50-mm narrow bore rapid resolution column (part# 871700-902, Agilent Technologies, Wilmington, DE). Separation was achieved using isocratic conditions, in a mobile phase of 70% acetonitrile containing 1% acetic acid at a flow rate of 0.25 mL/min. Eluted MePPEP was measured using an Agilent model 1946 single quad mass spectrometer run in positive mode, fitted with an electrospray ion source and set to *m/z* 455 ion. Clearly delineated chromatographic peaks with the retention time of authentic standards and expected molecular weight were seen after each injection of sample. Standards were prepared by adding known quantities of MePPEP to brain tissue samples from untreated rats and processed as described above. MePPEP was quantified based on peak area. Data are presented in ng MePPEP per g of tissue as mean±SD (n=3).

Compartmental modeling of rat with [^{11}C]MePPEP

To estimate the density of CB_1 receptors in brain, we performed compartmental modeling in 4 rats using 2-hour PET data and serial arterial plasma concentrations of [^{11}C]MePPEP separated from radiometabolites. We used measured values of the plasma concentration for all time points, since bi- and tri-exponential curves provided a poor fit of the plasma data. One and two-tissue compartmental models were analyzed with PMOD 2.85 software (PMOD Technologies Ltd., Adliswil, Switzerland). We followed the recently proposed consensus nomenclature for reversibly binding radioligands (Innis et al., 2007), where V_T is the total distribution volume, including specific and nondisplaceable uptake.

Measurement of parent and radiometabolites in plasma and brain

Anticoagulated blood samples (~1 mL for mouse, ~6 mL for rat) were obtained by cardiac puncture at 30 min after radioligand injection in mouse and after 30, 60, 90, and 120 min in rat. The animals were then euthanized by decapitation, and brain tissues were harvested. An additional blood sample was taken at 60 min from one rat that was euthanized at 120 min, and the plasma metabolite composition was found to match the other rats euthanized at 60 min. Thus, the rats euthanized at 120 min reliably reflect those euthanized at 60 min. We extracted, analyzed, and measured radioactivity in brain and plasma as described in Zoghbi et al. (2006). The HPLC used for these studies used a radial compression module (RCM-100) with a mobile phase of MeOH: H_2O:Et_3N (82.5:17.5:0.1; by volume) at a flow rate of 2.0 mL/min.

Concentrations of [^{11}C]MePPEP and radiometabolites were calculated as the product of the radio-HPLC fractional parent or radiometabolite activity multiplied by the total tissue activity (dpm/g). The recovery of added [^{11}C]MePPEP from plasma samples was >99%, and the recovery of total radioactivity from tissues and plasma samples was >83%. The recovery of radioactivity from HPLC column was monitored either by γ-counter measurements of the eluates or by injecting methanol (2 mL) at the end of analysis.

Results

Radioligand preparation

[^{11}C]MePPEP was prepared with 100±0% radiochemical purity, and 99.9±0% chemical purity. The specific activity at time of radioligand injection was 112.0±54.7 GBq/μmol (n=34 batches). The mean injected activity was 13.1±5.5 MBq (0.12±0.07 nmol) for mouse studies and 49.3±23 MBq (0.44±0.30 nmol) for rat studies.

Receptor occupancy by [^{11}C]MePPEP

Due to the relatively small body mass of rodents, PET ligands can cause significant (>5–10%) receptor occupancy, which violates the assumptions of tracer methodologies. We estimated the receptor occupancy in rodents caused by the injected mass dose of MePPEP based on reports of receptor density and on our measurements of brain uptake. The density (B_{max}) of CB_1 receptors in cerebellum is 1750 fmol per mg protein in rat (Hirst et al., 1996) and 1810 fmol per mg protein in mouse (Abood et al., 1997). Assuming that 10% of brain weight is protein, these densities correspond to 175 nM in rats and 181 nM in mice. The maximal brain uptake was ~190% SUV (2.4 nM) in rats and ~260% SUV (11.2 nM) in mice. Assuming that 80% of the ligand was specifically bound, the maximal occupancy of CB_1 receptors was 1.1% (=80%*2.4 nM/175 nM) in rats and 5.0% (=80%*11.2 nM/181 nM) in mice.

[^{11}C]MePPEP was not a P-gp substrate in mouse

[^{11}C]MePPEP was not a substrate for P-gp, an efflux transporter expressed at the blood-brain barrier. P-gp knockout (n=4) and wild

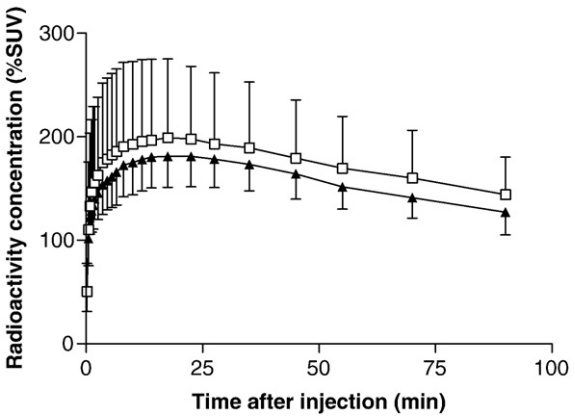

Fig. 1. Forebrain radioactivity after injecting [^{11}C]MePPEP in mice. Symbols represent the mean±SD for wild type (▲; n=4) and P-gp knockout (□; n=4) mice. The peak uptake was 199% SUV at 18 min in the knockout mice and 181% SUV at 18 min in the wild type mice.

Table 1
Effect of P-gp gene knockout on plasma and brain concentrations of [^{11}C]MePPEP in mice

Animal	[^{11}C]MePPEP concentration (% SUV)			
	C_P	Forebrain	Cerebellum	Forebrain/C_P
Wild type	5.5±4.8	191±56	214±63	65.0±55.2
P-gp knockout	8.2±0.8	373±146	383±160	44.8±13.0

C_P = plasma concentration of [^{11}C]MePPEP.

type (n=4) mice were injected with [^{11}C]MePPEP. Brain uptake peaked at ~20 min with similar concentrations of 200 and 182% SUV in the knockout and wild type mice, respectively (Fig. 1). In addition, the area under the curve of activity *vs.* time from 0 to 90 min in knockout mice was only 1.1 times that of wild type mice with no significant difference between the two groups (P=0.58, two-tailed Student t-test).

To determine whether greater brain uptake in P-gp knockout than in wild type mice was merely the result of higher plasma concentration of the radioligand, we euthanized animals at 30 min and measured radioactivity in brain and plasma. The concentrations of [^{11}C]MePPEP in plasma were 5.5 and 8.2% SUV for wild type and P-gp knockout mice, respectively, with corresponding forebrain uptake of 191 and 383% SUV (Table 1). The brain to plasma ratio at this single time point was actually lower in P-gp knockout (45) compared to wild type (65) mice, on average. Thus, [^{11}C]MePPEP was not a substrate for P-gp in mice as assessed with brain uptake, either corrected or uncorrected for the plasma concentration of radioligand.

Specificity of [^{11}C]MePPEP for CB$_1$ receptors in mice

[^{11}C]MePPEP was selective for the CB$_1$ receptor in mice when assessed by pharmacological displacement of a highly selective CB$_1$ inverse agonist. Baseline and displacement scans were acquired within a 3-hour interval in the same animal. Rimonabant (3 mg/kg IV), administered at 25 min after [^{11}C]MePPEP, displaced more than half of the brain activity by 90 min compared to the baseline scan. After displacement by rimonabant, brain uptake decreased from peak of 260% at 25 min to about 100% SUV at 90 min. The residual activity after displacement was similar to that of a preblock study in a different animal (Fig. 2A). In the preblock study, the same dose of rimonabant was given at 30 min before [^{11}C]MePPEP. A ratio of areas under the curve of preblocked *vs.* baseline animals from 0 to 90 min was 0.32, indicating that 68% of brain uptake was specifically bound to CB$_1$ receptors.

Comparing CB$_1$ knockout to wild type mice with [^{11}C]MePPEP yielded results of receptor selectivity consistent with the displacement by rimonabant. Brain activity in CB$_1$ receptor knockout mice was 100% SUV at 3 min and quickly declined to 30% SUV at 90 min. In contrast, maximal brain uptake in wild type animals was 170% SUV at 20 min and slowly declined to 100% SUV at 90 min (Fig. 2B). Thus, compared to knockout animals, the CB$_1$ receptors in the wild type mice bound more radioligand and therefore required greater time to achieve peak activity in brain. The ratio of

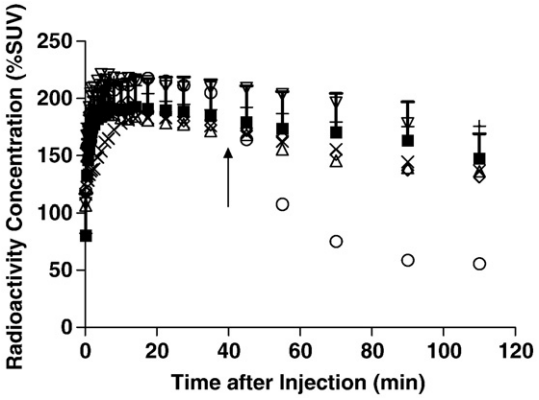

Fig. 3. Displacement of [^{11}C]MePPEP by agonists and inverse agonist in rats. Drugs were administered IV 40 min after [^{11}C]MePPEP. Anandamide (△) 10 mg/kg; methanandamide (▽) 10 mg/kg; CP 55,940 (◊) 1 mg/kg; URB597 (anandamide reuptake inhibitor, ×) 0.6 mg/kg; URB597 with anandamide (+) 0.6 mg/kg and 10 mg/kg, respectively; and rimonabant (○) 3 mg/kg. The curves are representative of two studies with anadamide, CP 55,940, URB597 both alone and with anandamide, and rimonabant, and of one study with methanandamide. The baseline curve (■) is the mean of 8 animals.

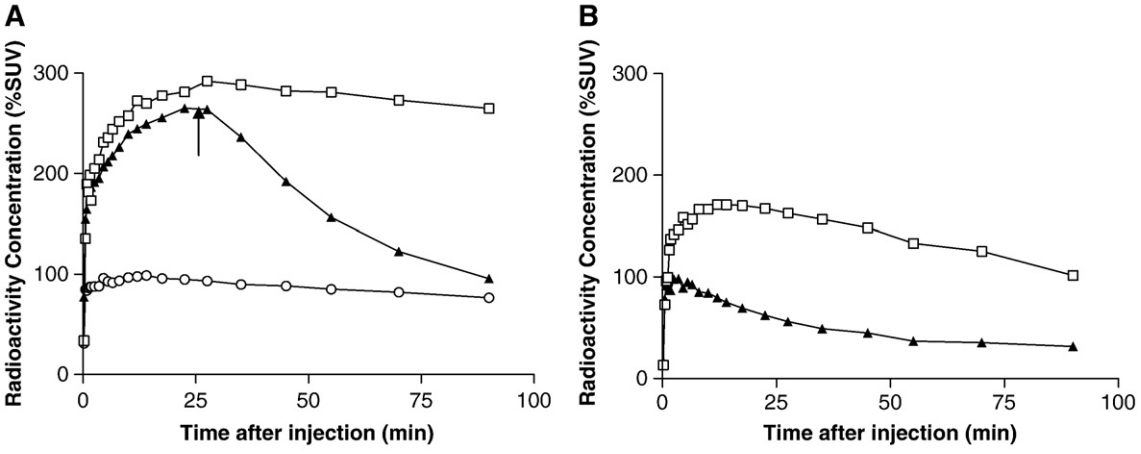

Fig. 2. Displacement of brain activity in P-gp knockout and CB$_1$ receptor knockout mice. (A) P-gp knockout mice were examined under baseline (□), displacement (▲), and preblocked (○) conditions. Rimonabant (3 mg/kg, IV) was administered 30 min before or 25 min (↑) after [^{11}C]MePPEP. (B) Forebrain time-activity curves in a wild type (□) and CB$_1$ receptor knockout (▲) mouse.

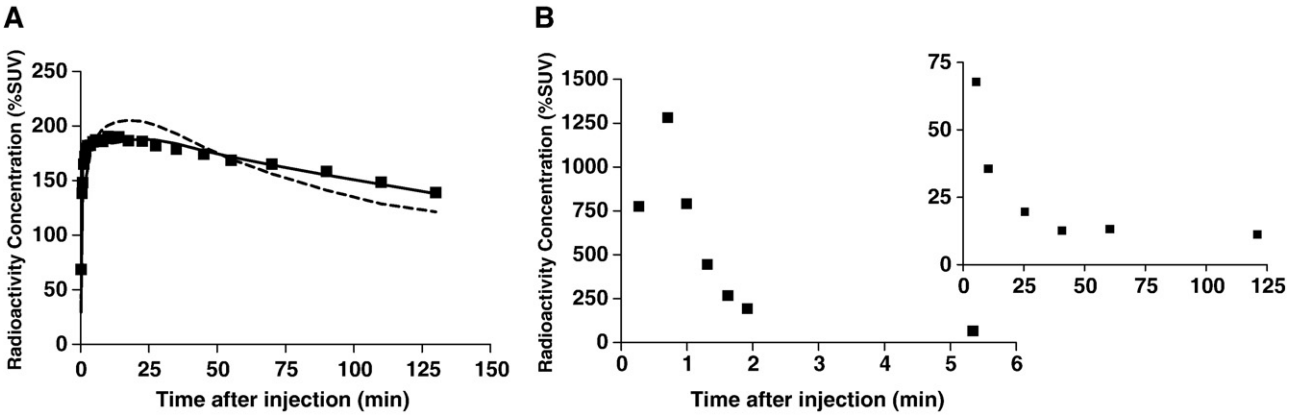

Fig. 4. Brain and plasma concentrations of radioactivity after injecting [^{11}C]MePPEP in rats. (A) The brain time-activity curve of this rat was visually and statistically better fit by the two- (solid line) than the one- (dashed line) tissue compartment model. ($P=0.007$ by F-test). (B) The plasma concentration of [^{11}C]MePPEP separated from radiometabolites from same animal as panel A peaked at 45 s and rapidly declined thereafter. The range of the concentration was large, and the insert has an overlapping value at 5 min.

areas under the curve from 0 to 90 min in knockout compared to wild type mice was 0.35, indicating that 65% of the uptake was specifically bound to CB_1 receptors.

Displacement by agonists vs. inverse agonists

Direct and indirect acting agonists caused no discernable changes in brain uptake (Fig. 3), and all agonist curves at their terminal points were within one standard deviation of baseline scans ($n=8$). The direct acting agonists anandamide (10 mg/kg IV, $n=2$), methanandamide (10 mg/kg IV, $n=1$), and CP 55,940 (1 mg/kg IV, $n=2$) were administered at 40 min. Inhibition of anandamide reuptake by inhibiting both FAAH, the enzyme that metabolizes anandamide, and the anandamide transporter has an indirect agonist effect by increasing the concentration of this endocannabinoid. The anandamide reuptake process blocker, URB597, was administered at 40 min after radioligand injection in two animals (0.3 mg/kg and 0.6 mg/kg IV), and as a pretreatment at 1 h before radioligand injection in a third animal (0.3 mg/kg IV). Two additional animals were pretreated with URB597 (0.6 mg/kg IV), and anandamide (10 mg/kg IV) was administered 40 min after radioligand injection.

The direct agonist agents were administered at doses that had pharmacological effects. Anandamide transiently decreased respiration rate, with shallow and irregular breathing. Methanandamide caused the death of one animal after 35 min, possibly by respiratory depression. CP 55,940 caused decreased respiration rate for the duration of the scan, and later the death of one animal after 50 min. In contrast, URB597 had no noticeable pharmacological effect.

In contrast to the agonists, rimonabant rapidly displaced brain activity when administered at 3 mg/kg IV at 40 min after the radioligand ($n=2$ rats). Compared to baseline studies ($n=8$ rats), rimonabant decreased brain activity by 63% at the end of the scan (2 h) (Fig. 3). Rimonabant had no noticeable effects on temperature or respiration.

Ex vivo mass spectrometry

Our results of agonist state assessment using PET were reliably replicated using *ex vivo* mass spectrometry. Rimonabant (an inverse agonist) caused >90% receptor blockade, whereas CP 55,940 (an agonist) caused no receptor blockade. More specifically, rimonabant (10 mg/kg) pretreatment decreased MePPEP in rat frontal cortex at 60 min from a baseline, vehicle-treated concentration of 34.4±5.3 to 2.3±0.6 ng/g. In contrast, CP 55,940 (1 mg/kg) caused no significant change in the concentration of MePPEP against vehicle-treated rats from 40.0±4.4 to 40.3±1.5 ng/g. Rimonabant appeared to displace or block more MePPEP binding measured by *ex vivo* mass spectrometry (>90%) than by *in vivo* PET (~65%).

Compartmental modeling of [^{11}C]MePPEP in rat brain

Pharmacokinetic modeling of brain and plasma time-activity data showed that estimates of total distribution volume (V_T) achieved stable, well identified values during a 2-hour scan. We used brain time-activity data and serial plasma concentrations of [^{11}C]MePPEP to estimate V_T, which is proportional to receptor density (B_{max}). Due to the limited resolution of PET, the measured concentrations of brain activity were similar in all regions. For this reason, we sampled activity from a large area that included the entire forebrain.

In three out of four rodents the two-tissue compartment model was superior to the one-tissue compartmental model, and we used both to assess the minimal imaging time required for stable identification of V_T. The brain time-activity data from 0–120 min ($n=4$ rats) as well as the measured serial concentration of [^{11}C]MePPEP were analyzed with compartmental modeling. The two-tissue compartment model gave better statistical fit of brain data than the one-tissue compartment in three of the four rats with $P<0.01$, with the other animal achieving $P=0.08$ (F-test; Fig. 4A). To assess the stability of distribution volume over time, we increasingly truncated the brain data, from 0–120 to 0–30 min, at terminal times of 120, 100, 80, 60, 50, 40, and 30 min. The calculated distribution volume increased asymptotically from 30 to 120 min and reached 90% of the terminal value within ~70 and 55 min for one-tissue and two-tissue compartmental models, respectively (Fig. 5).

The concentration of unchanged [^{11}C]MePPEP rapidly declined in plasma. From a peak of ~1100% SUV at about 45 s, its

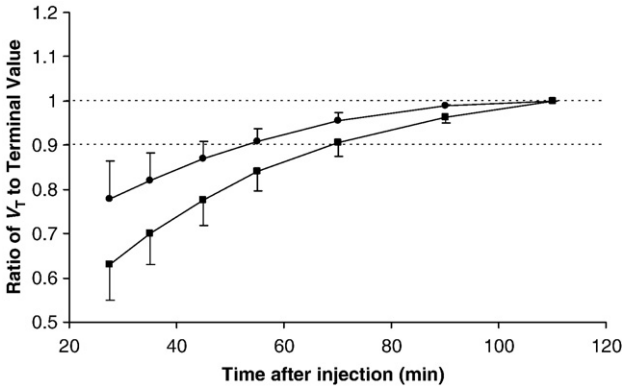

Fig. 5. Time instability of distribution volume (V_T) in rat. Increasingly truncated intervals of brain time-activity data were analyzed from time 0 to that indicated on the *x*-axis. Time points represent the mid-point of the acquisition time, therefore data captured in a time frame from 100 to 120 min are plotted at 110 min. V_T was calculated for one-(■) and two-(●) tissue compartment models and expressed as a ratio to that determined with the complete scanning data from 0 to 120 min. The terminal V_T for forebrain was 9.4±3.7 mL cm^{-3} for one-tissue and 10.0±4.2 mL cm^{-3} for two-tissue compartment models. The error bar represents SD of the ratios, n=4 animals.

concentration declined to 50% SUV at 5 min and further to 12% SUV at 120 min (Fig. 4B). Metabolism was also rapid, as shown by the accumulation of radiometabolites in plasma. [^{11}C]MePPEP as a percentage of total radioactivity declined from 100% in the injected sample to 50±9.1% at 5 min, 27±5.8% at 26 min, and 16±1.5% at 60 min (Fig. 6A). Rat plasma samples contained at least three radiometabolites, which eluted earlier than [^{11}C]MePPEP on HPLC and were, therefore, less lipophilic than the parent radioligand (Fig. 6B).

Ex vivo measurements in rat

To assess the chemical composition of radioactivity in brain over time, we euthanized three animals at 30, 60, and 90 min, and two animals at 120 min. Radiometabolites of [^{11}C]MePPEP were present in rat brain but at relatively stable percentage (~13%) of total radioactivity. The percentages of radiometabolites in rat brain were 12.9±0.4% at 30 min, 13.2±6.0% at 60 min, 16.4±9.3% at 90 min, and 12.3±4.8% at 120 min.

Discussion

[^{11}C]MePPEP was not a substrate for P-gp in mice, and was selective for the CB_1 receptor based on displacement studies in rats and on imaging of receptor knockout mice. In both rodent species, specific binding was ~65% of total brain uptake. Although the inverse agonist rimonabant displaced [^{11}C]MePPEP, agonists at high doses were ineffective (anandamide, methanandamide, CP 55,940, and URB597). Compartmental modeling in rats showed that distribution volume was defined within 90% of the value at 120 min within 70 min of scanning. Distribution volume is the ratio at equilibrium of the drug concentration in brain to that plasma. Since we estimated total radioactivity with PET rather than only unchanged [^{11}C]MePPEP, we overestimated its distribution volume in rat brain by ~13%.

Utility of PET imaging in rodents

PET is an expensive methodology and arguably should be reserved for human experimentation or studies preliminary for such use. With this perspective, what are the advantages and disadvantages of using rodents to screen radioligand candidates and to understand their distribution in the body?

P-gp and other efflux transporters have been increasingly recognized over the past 10–20 years to modulate the distribution and metabolism of many drugs (Ambudkar et al., 1999). P-gp inhibitors can be used to assess whether a drug is a substrate, but these inhibitors may have secondary effects that confound the primary measurement. Cyclosporin A is a so-called "first generation" P-gp inhibitor and has multiple other effects on drug disposition and general health of the animal (Liow et al., 2007). In contrast to pharmacological inhibition, P-gp knockout mice provide an exact genetic model. Nevertheless, results from these transgenic animals should be interpreted cautiously. P-gp shows a species difference in substrate selectivity, and results in rodents may not apply in primates (Katoh et al., 2006). In addition, P-gp is

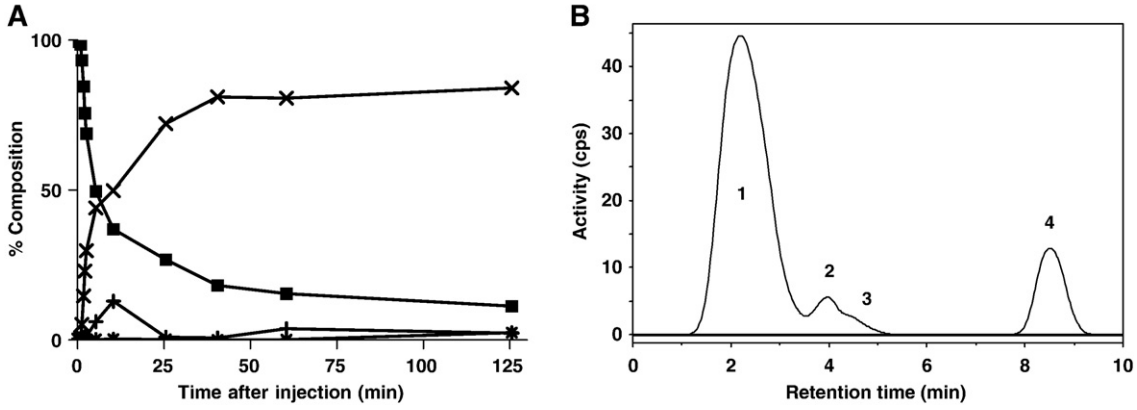

Fig. 6. Metabolism of MePPEP in rat. (A) Metabolism of MePPEP (■) was rapid with most of the radioactivity comprised of the most polar metabolite (×) by the end of the scan. The curves represent the mean of 4 animals. (B) At 90 min three metabolites less lipophilic than MePPEP were eluted by HPLC. The most polar metabolite (1) was followed by two more lipophilic metabolites (2 and 3), separated from MePPEP (4). This representative chromatograph comes from a single animal.

widespread in the body and can affect metabolism and distribution. Thus, control experiments are indicated, as we performed for [^{11}C]MePPEP (Table 1), to ensure that the effects on brain uptake are not merely mediated by changes in plasma concentration of radioligand.

Similar to secondary effects of pharmacological inhibition of P-gp, CB_1 receptor displacing agents may also have off-target activity. The CB_1 receptor knockout mouse provides a highly specific model of receptor blockade. Combined use of this transgenic animal with pharmacological displacement provided definitive evidence that the *in vivo* brain uptake of [^{11}C]MePPEP was selective and specific for the CB_1 receptor. In addition, we found that the nonspecific uptake was ~35% in both CB_1 receptor knockout mice and rimonabant-treated mice and rats.

PET measures only radio activity and does not identify its chemical source e.g., parent *vs.* radiometabolite. Thus, one advantage of rodent imaging is the ease of sacrificing the animal to identify radiochemical species. For example, increasing distribution volume with time in monkeys and humans is often interpreted as evidence for accumulation of radiometabolites in brain. We extracted radioactivity from rat brain at several times after radioligand injection and characterized its radiochemical composition with HPLC. Our data showed that radiometabolites in brain could account for the delay in reaching an accurate distribution volume during the period 30 to 120 min.

Experiments with rodents can use high doses of drugs that would be toxic to monkeys or not approved for humans. For example, we used high and toxic doses of CB_1 receptor ligands to estimate maximal displacement of [^{11}C]MePPEP in brain. Doses were selected (see Materials and methods) that were active by behavioral testing (e.g., methanandamide) or by measurement of increased anandamide concentrations in brain (e.g., the anandamide reuptake process inhibitor, URB597). Furthermore, the doses were toxic (anandamide) and even fatal in two situations (methanandamide, CP 55,940; see Results).

Two limitations of PET imaging in rodents relate to the small size of their brains, which affects both resolution and the maximal mass dose of carrier ligand that may be given without causing unacceptable receptor occupancy. The resolution of PET cameras for small animals is ~1.5 mm, while those for humans have resolutions of 2.5 to 6 mm (Cherry, 2006). The rat brain (~1.5 g) is >900 times smaller than that of humans (~1400 g), which correlates to a decrease in spherical radius by ~10 fold. Therefore, although the resolution of rodent PET is 2 to 4 times better than primate PET, the distance between brain structures is about 10 times smaller. Even the enhanced resolution that may be achieved by placing detectors close to the rodent brain does not compensate for the much smaller size of the target. Thus, one cannot reliably measure substructures in rodent brain as in humans.

The small size of the rodent brain also imposes strict limits on injected mass dose of carrier ligand. For example, the same mass dose of ligand will occupy a higher percentage of CB_1 receptors in mice than in humans, because mice have fewer receptors. The concentration of receptors may be similar, but the volume in mice is smaller than in humans. Radioligand imaging is typically performed under tracer conditions, in which 5–10% of receptors are occupied by carrier ligand. Greater occupancies violate the assumptions of compartmental modeling and typically preclude measurement of distribution volume. Thus, one must confirm that doses which provide tracer receptor occupancy in humans are appropriate for rodents. For [^{11}C]MePPEP, we extracted brain radioactivity and, based on published values of receptor density, estimated that the peak concentration of radioligand corresponds to <1.1% and <5% receptor occupancy in rat and mouse brain, respectively.

Utility of ex vivo mass spectrometry

Mass spectrometry has several advantages relative to PET and can be used to select candidates for PET scanning. Compared to PET, *ex vivo* mass spectrometry is rapid, can study a large group of animals and several displacing agents in one day, does not involve radioactivity or require a cyclotron, and may be set to measure the parent compound only. In fact, we had used *ex vivo* mass spectrometry to compare potency and time course of receptor occupancy by a number of candidates prior to selecting MePPEP for radiolabeling and PET imaging. Although mass spectrometry has the advantage of monitoring a single identified chemical species, the results do not necessarily reflect those from PET, which measures total radioactivity comprised of parent radioligand and radiometabolites. For example, in the current study, *ex vivo* mass spectrometry showed that rimonabant displaced >90% of MePPEP brain uptake, whereas comparable PET imaging showed that rimonabant displaced ~65% of brain radioactivity after injection of [^{11}C]MePPEP. The difference was caused in part by radiometabolites measured with PET that were not detected with mass spectrometry.

Displacement of an inverse agonist radioligand by agonists ligands

We found that agonists were much less potent than inverse agonists to displace [^{11}C]MePPEP binding to CB_1 receptors in rat brain. Our results cannot distinguish between two potential and previously published explanations: receptor reserve and non-overlapping binding sites. The situation is complex because of potential differences with *in vitro* and *in vivo* binding and the unclear mechanism of inverse agonism.

First, we should distinguish *in vitro* affinity and *in vivo* receptor occupancy. *In vitro* binding studies have shown that the agonists we used have 2–100 fold lower affinity than rimonabant for CB_1 receptors. For example, anandamide and methanandamide have 2–10 fold lower affinity than rimonabant to displace the agonist ligand [^{3}H]CP 55940 (Abadji et al., 1994, Adams et al., 1995, 1998). In addition, anandamide has 100 fold lower affinity than rimonabant to displace [^{3}H]rimonabant itself (Rinaldi-Carmona et al., 1996). Although these two agonists have clearly lower *in vitro* receptor affinity than rimonabant, the question we have addressed is the *in vivo* occupancy associated with pharmacological effects.

Second, the mechanism of inverse agonism is not completely understood, and its expression is dependent upon the particular assay system (Pertwee, 2005). Nevertheless, inverse agonists universally antagonize (*i.e.*, reverse) the effects of agonists. The special property of inverse agonists is their ability, in at least some systems, to reduce the output signal below baseline levels found in the absence of agonist. Rinaldi-Carmona et al. (1996) studied the binding of [^{3}H]rimonabant, an inverse agonist. They found that some agonists, like CP 55,940 and WIN 55,212-2, had competitive inhibition but that the endogenous cannabinoid, anandamide, had noncompetitive/allosteric effects. Furthermore, receptor mutational analysis and molecular modeling support separate or partially overlapping binding sites for agonists, inverse agonists, and anandamide (McAllister et al., 2003; Murphy and Kendall, 2003). Thus, one explanation for our finding of minimal potency of agonists to displace [^{11}C]

MePPEP is that the agonist site does not completely overlap with the inverse agonist site labeled by [^{11}C]MePPEP.

Using an *in vitro* system, Gifford et al. (1999) suggested that CB_1 receptors have significant receptor reserve for agonists. They used superfused rat hippocampal slices and electrically-evoked [^{3}H]acetylcholine release to assay the CB_1 receptor for a dose-response. The agonist WIN 55,212-2 maximally inhibited acetylcholine release at only 7.5% occupancy of [^{131}I]AM 281-labeled receptors. These results were interpreted as receptor reserve, in which maximal agonist effect is achieved at much less than full receptor occupancy.

Our PET imaging results cannot determine whether the inability of CB_1 agonist ligands to displace [^{11}C]MePPEP is due to high receptor reserve or non-overlapping agonist and inverse agonist binding sites. An agonist PET radioligand would provide valuable information, and our studies show that rodents can be used with PET to measure *in vivo* CB_1 receptor binding.

Conclusion

Using pharmacological displacements and knockout mice, we found that [^{11}C]MePPEP was selective for the CB_1 receptor and had specific binding representing ~65% of total brain radioactivity. The much higher *in vivo* potency of inverse agonists *vs.* agonists to displace [^{11}C]MePPEP is consistent with these two binding sites being non-overlapping or with significant receptor reserve for agonist effects. Rat brain contained ~13% radiometabolites from 30 to 120 min, which thereby overestimated distribution volume to a similar extent.

Acknowledgments

We thank Jinsoo Hong and Cheryl Morse for the radioligand preparation; Jonathan P. Gourley and Ed Tuan for their help with radiometabolite analysis; Drs. Fumihiko Yasuno and Masao Imaizumi for their assistance with PET imaging; and PMOD Technologies for providing its image analysis and modeling software.

This research was performed via a Cooperative Research and Development Agreement with Eli Lilly, Karolinska Institutet, and NIMH. These studies were supported by the Intramural Program of NIMH (project Z01-MH-002795-04) and research support from Eli Lilly.

References

Abadji, V., Lin, S., Taha, G., Griffin, G., Stevenson, L.A., Pertwee, R.G., Makriyannis, A., 1994. (*R*)-methanandamide: a chiral novel anandamide possessing higher potency and metabolic stability. J. Med. Chem. 37, 1889–1893.

Abood, M.E., Ditto, K.E., Noel, M.A., Showalter, V.M., Tao, Q., 1997. Isolation and expression of a mouse CB_1 cannabinoid receptor gene. Comparison of binding properties with those of native CB_1 receptors in mouse brain and N18TG2 neuroblastoma cells. Biochem. Pharmacol. 53, 207–214.

Adams, I.B., Ryan, W., Singer, M., Thomas, B.F., Compton, D.R., Razdan, R.K., Martin, B.R., 1995. Evaluation of cannabinoid receptor binding and *in vivo* activities for anandamide analogs. J. Pharmacol. Exp. Ther. 273, 1172–1181.

Adams, I.B., Compton, D.R., Martin, B.R., 1998. Assessment of anandamide interaction with the cannabinoid brain receptor: SR 141716A antagonism studies in mice and autoradiographic analysis of receptor binding in rat brain. J. Pharmacol. Exp. Ther. 284, 1209–1217.

Ambudkar, S.V., Dey, S., Hrycyna, C.A., Ramachandra, M., Pastan, I., Gottesman, M.M., 1999. Biochemical, cellular, and pharmacological aspects of the multidrug transporter. Annu. Rev. Pharmacol. Toxicol. 39, 361–398.

Burns, H.D., Van Laere, K., Sanabria-Bohorquez, S., Hamill, T.G., Bormans, G., Eng, W.S., Gibson, R., Ryan, C., Connolly, B., Patel, S., Krause, S., Vanko, A., Van Hecken, A., Dupont, P., De Lepeleire, I., Rothenberg, P., Stoch, S.A., Cote, J., Hagmann, W.K., Jewell, J.P., Lin, L.S., Liu, P., Goulet, M.T., Gottesdiener, K., Wagner, J.A., de Hoon, J., Mortelmans, L., Fong, T.M., Hargreaves, R.J., 2007. [^{18}F]MK-9470, a positron emission tomography (PET) tracer for *in vivo* human PET brain imaging of the cannabinoid-1 receptor. Proc. Natl. Acad. Sci. U. S. A. 104, 9800–9805.

Chernet, E., Martin, L.J., Li, D., Need, A.B., Barth, V.N., Rash, K.S., Phebus, L.A., 2005. Use of LC/MS to assess brain tracer distribution in preclinical, *in vivo* receptor occupancy studies: dopamine D_2, serotonin 2A and NK-1 receptors as examples. Life Sci. 78, 340–346.

Cherry, S.R., 2006. The 2006 Henry N Wagner lecture: of mice and men (and positrons)—advances in PET imaging technology. J. Nucl. Med. 47, 1735–1745.

Dickason-Chesterfield, A.K., Kidd, S.R., Moore, S.A., Schaus, J.M., Liu, B., Nomikos, G.G., Felder, C.C., 2006. Pharmacological characterization of endocannabinoid transport and fatty acid amide hydrolase inhibitors. Cell Mol. Neurobiol. 26, 407–423.

Fride, E., Mechoulam, R., 1993. Pharmacological activity of the cannabinoid receptor agonist, anandamide, a brain constituent. Eur. J. Pharmacol. 231, 313–314.

Gifford, A.N., Bruneus, M., Gatley, S.J., Lan, R., Makriyannis, A., Volkow, N.D., 1999. Large receptor reserve for cannabinoid actions in the central nervous system. J. Pharmacol. Exp. Ther. 288, 478–483.

Grotenhermen, F., 2005. Cannabinoids. Curr. Drug Targets CNS Neurol. Disord. 4, 507–530.

Hirst, R.A., Almond, S.L., Lambert, D.G., 1996. Characterisation of the rat cerebella CB_1 receptor using SR141716A, a central cannabinoid receptor antagonist. Neurosci Lett. 220, 101–104.

Innis, R.B., Cunningham, V.J., Delforge, J., Fujita, M., Gjedde, M., Gunn, R.N., Holden, J., Houle, S., Huang, S.C., Ichise, M., Iida, H., Ito, H., Kimura, Y., Koeppe, R.A., Knudsen, G.M., Knuuti, J., Lammertsma, A.A., Laruelle, M., Logan, J., Maguire, R.P., Mintun, M.A., Morris, E.D., Parsey, R., Price, J.C., Slifstein, M., Sossi, V., Suhara, T., Votaw, J.R., Wong, D.F., Carson, R.E., 2007. Consensus nomenclature for *in vivo* imaging of reversibly binding radioligands. J. Cereb. Blood Flow Metab. 27, 1533–1539.

Johnson, C.A., Seidel, J., Vaquero, J.J., Pascau, J., Desco, M., Green, M.V., 2002. Exact positioning for OSEM reconstructions on the ATLAS depth-of-interaction small animal scanner. Mol. Imaging Biol. 4, S22.

Katoh, M., Suzuyama, N., Takeuchi, T., Yoshitomi, S., Asahi, S., Yokoi, T., 2006. Kinetic analyses for species differences in P-glycoprotein-mediated drug transport. J. Pharm. Sci. 95, 2673–2683.

Liow, J., Seidel, J., Johnson, C.A., Toyama, H., Green, M.V., Innis, R.B., 2003. A single slice rebinning/2D exact positioning OSEM reconstruction for the NIH ATLAS small animal PET scanner. J. Nucl. Med. 44 163P.

Liow, J.S., Lu, S., McCarron, J.A., Hong, J., Musachio, J.L., Pike, V.W., Innis, R.B., Zoghbi, S.S., 2007. Effect of a P-glycoprotein inhibitor, Cyclosporin A, on the disposition in rodent brain and blood of the 5-HT_{1A} receptor radioligand, [^{11}C](*R*)-(−)-RWAY. Synapse. 61, 96–105.

McAllister, S.D., Rizvi, G., Anavi-Goffer, S., Hurst, D.P., Barnett-Norris, J., Lynch, D.L., Reggio, P.H., Abood, M.E., 2003. An aromatic microdomain at the cannabinoid CB_1 receptor constitutes an agonist/inverse agonist binding region. J. Med. Chem. 46, 5139–5152.

McGregor, I.S., Issakidis, C.N., Prior, G., 1996. Aversive effects of the synthetic cannabinoid CP 55,940 in rats. Pharmacol. Biochem. Behav. 53, 657–664.

Murphy, J.W., Kendall, D.A., 2003. Integrity of extracellular loop 1 of the human cannabinoid receptor 1 is critical for high-affinity binding of the ligand CP 55,940 but not SR 141716A. Biochem. Pharmacol. 65, 1623–1631.

Pacher, P., Batkai, S., Kunos, G., 2006. The endocannabinoid system as an emerging target of pharmacotherapy. Pharmacol Rev. 58, 389–462.

Paxinos, G., Watson, C., 1998. The Rat Brain in Stereotaxic Coordinates, 4th ed. Academic Press, New York.

Paxinos, G., Franklin, K.B.J., 2001. The Mouse Brain in Stereotaxic Coordinates. Academic Press, San Diego.

Pertwee, R.G., 2005. Inverse agonism and neutral antagonism at cannabinoid CB_1 receptors. Life Sci. 76, 1307–1324.

Piomelli, D., Tarzia, G., Duranti, A., Tontini, A., Mor, M., Compton, T.R., Dasse, O., Monaghan, E.P., Parrott, J.A., Putman, D., 2006. Pharmacological profile of the selective FAAH inhibitor KDS-4103 (URB597). CNS Drug Rev. 12, 21–38.

Rinaldi-Carmona, M., Pialot, F., Congy, C., Redon, E., Barth, F., Bachy, A., Breliere, J.C., Soubrie, P., Le Fur, G., 1996. Characterization and distribution of binding sites for [^{3}H]-SR 141716A, a selective brain (CB_1) cannabinoid receptor antagonist, in rodent brain. Life Sci. 58, 1239–1247.

Schinkel, A.H., Wagenaar, E., Mol, C.A., van Deemter, L., 1996. P-glycoprotein in the blood-brain barrier of mice influences the brain penetration and pharmacological activity of many drugs. J. Clin Invest. 97, 2517–2524.

Seidel, J., Vaquero, J.J., Green, M.V., 2003. Resolution uniformity and sensitivity of the NIH ATLAS small animal PET scanner: comparison to simulated LSO scanners without depth-of-interaction capability. IEEE Trans. Nucl. Sci. 50, 1347–1350.

Van Gaal, L.F., Rissanen, A.M., Scheen, A.J., Ziegler, O., Rossner, S., 2005. Effects of the cannabinoid-1 receptor blocker rimonabant on weight reduction and cardiovascular risk factors in overweight patients: 1-year experience from the RIO-Europe study. Lancet 365, 1389–1397.

Xie, S., Furjanic, M.A., Ferrara, J.J., McAndrew, N.R., Ardino, E.L., Ngondara, A., Bernstein, Y., Thomas, K.J., Kim, E., Walker, J.M., Nagar, S., Ward, S.J., Raffa, R.B., 2007. The endocannabinoid system and rimonabant: a new drug with a novel mechanism of action involving cannabinoid CB_1 receptor antagonism–or inverse agonism–as potential obesity treatment and other therapeutic use. J. Clin. Pharm. Ther. 32, 209–231.

Yasuno, F., Brown, A.K., Zoghbi, S.S., Krushinski, J.H., Chernet, E., Tauscher, J., Schaus, J.M., Phebus, L.A., Chesterfield, A.K., Felder, C.C., Gladding, R.L., Hong, J., Halldin, C., Pike, V.W., Innis, R.B., 2008. The PET radioligand [^{11}C]MePPEP binds reversibly and with high specific signal to cannabinoid CB_1 receptors in nonhuman primate brain. Neuropsychopharmacology 33, 259–269.

Zoghbi, S.S., Shetty, H.U., Ichise, M., Fujita, M., Imaizumi, M., Liow, J.S., Shah, J., Musachio, J.L., Pike, V.W., Innis, R.B., 2006. PET imaging of the dopamine transporter with ^{18}F-FECNT: a polar radiometabolite confounds brain radioligand measurements. J Nucl Med. 47, 520–527.